Supplemental Information for

Isotopic measurements in water vapor, precipitation, and seawater during EUREC^{4}A

Adriana Bailey[1], Franziska Aemisegger[2], Leonie Villiger[2], Sebastian A. Los[3], Gilles Reverdin[4], Estefanía Quiñones Meléndez[5], Claudia Acquistapace[6], Dariusz B. Baranowski[7], Tobias Böck[6], Sandrine Bony[8], Tobias Bordsdorff[9], Derek Coffman[10], Simon P. de Szoeke[5], Christopher J. Diekmann[11,12], Marina Dütsch[13,14], Benjamin Ertl[11,15], Joseph Galewsky[3], Dean Henze[5], Przemyslaw Makuch[16], David Noone[17,5], Patricia K. Quinn[10], Michael Rösch[18], Andreas Schneider[9,19], Matthias Schneider[11], Sabrina Speich[20], Bjorn Stevens[21], Elizabeth J. Thompson[22]

[1]National Center for Atmospheric Research, Boulder, CO, USA
[2]Institute for Atmospheric and Climate Science, ETH Zurich, Zurich, Switzerland
[3]Department of Earth & Planetary Sciences, University of New Mexico, Albuquerque, NM, USA
[4]Laboratoire d'Océanographie et du Climat: expérimentation et approches numériques (LOCEAN/IPSL), Sorbonne Université-CNRS-IRD-MNHN, Paris, France
[5]College of Earth, Ocean, and Atmospheric Sciences, Oregon State University, Corvallis, OR, USA
[6]Institute for Geophysics and Meteorology, University of Cologne, Köln, Germany
[7]Institute of Geophysics Polish Academy of Sciences, Warsaw, Poland
[8]Laboratoire de Météorologie Dynamique (LMD/IPSL), CNRS, Sorbonne University, Paris, France
[9]Netherlands Institute for Space Research, SRON, Leiden, the Netherlands
[10]NOAA Pacific Marine Environmental Laboratory (PMEL), Seattle, WA, USA
[11]Institute of Meteorology and Climate Research (IMK-ASF), Karlsruhe Institute of Technology (KIT), Karlsruhe, Germany
[12]now at Telespazio Germany GmbH, Darmstadt, Germany
[13]University of Vienna, Vienna, Austria
[14] University of Washington, Seattle, WA, USA
[15]Steinbuch Centre for Computing (SCC), Karlsruhe Institute of Technology (KIT), Karlsruhe, Germany
[16]Institute of Oceanology Polish Academy of Sciences, Sopot, Poland
[17]Department of Physics, University of Auckland, Auckland, New Zealand
[18]Department of Environmental Systems Science, ETH Zurich, Zurich, Switzerland
[19]Finnish Meteorological Institute, Sodankylä, Finland
[20]LMD/IPSL, École Normale Supérieure, CNRS, Paris, France
[21]Max Planck Institute for Meteorology, Hamburg, Germany
[22]NOAA Physical Sciences Laboratory, Boulder, CO, USA

Correspondence to: Adriana Bailey (abailey@ucar.edu)

Contents

Text S3	P-3 calibration results and uncertainty estimates
Table S1	Liquid standard values and their uncertainties for Meteor water vapor measurements
Figure S7	Meteor quality control flags

Introduction

This supplement provides additional information about the sampling designs, calibration procedures, post-processing, and/or uncertainty estimates for water vapor isotopic measurements made at the Barbados Cloud Observatory (BCO), aboard the ATR aircraft, aboard the P-3 aircraft, and aboard the Meteor.

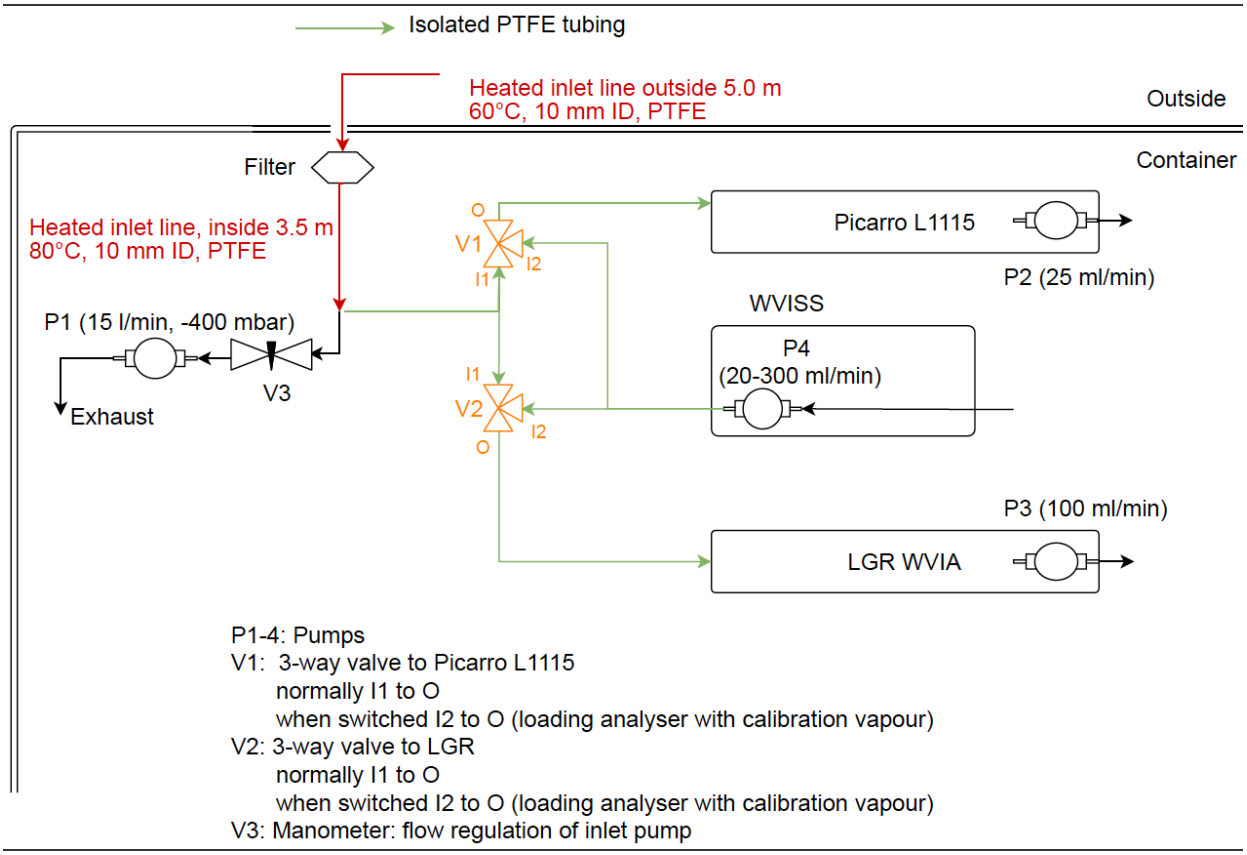

Figure S1: BCO sampling schematic. Red arrows depict the heated 12 mm OD line through which a KNF pump (HN022AN.18) pulled ambient air into the instrument container at a rate of 15 L min^{-1}. Green arrows depict the isolated ¼ inch OD PTFE tubing through which the two water vapor isotopic analyzers – a Picarro L1115 analyzer using cavity ringdown spectroscopy (CRDS) and a Los Gatos Research (LGR) analyzer using off-axis integrated cavity output spectroscopy (OA-ICOS) – picked off sub-samples of the main flow at rates of 0.025 and 0.1 L min^{-1}, respectively. Three-way valves (labeled V1 and V2) allowed the analyzers to alternate between measuring ambient water vapor and calibration gases, which were generated using an LGR water vapor isotope standard source (WVISS).

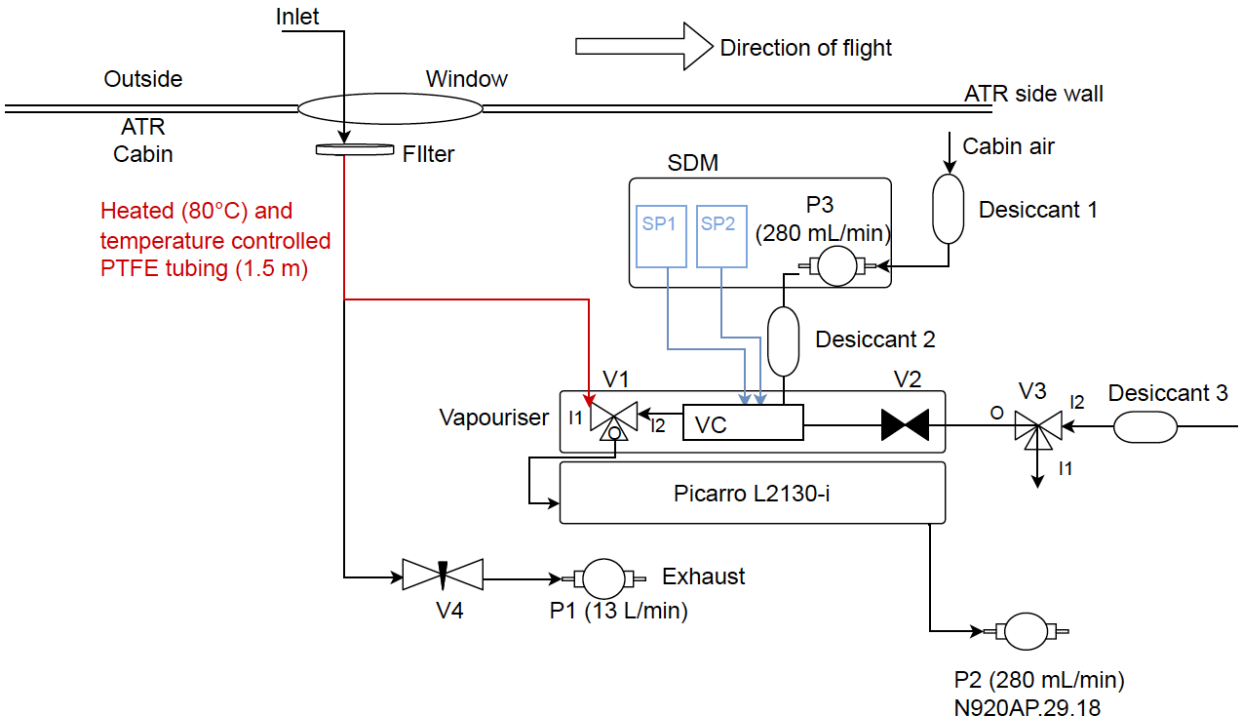

P1-3: Pumps
VC: Vapouriser chamber for standard gas sample preparation
V1: 3-way valve in vapouriser
normally I1 to O
when switched I2 to O (loading analyser (valve mask 14)
V2: normally closed valve
when switched vacuum overflow during sample preparation for calibration (valve mask 2)
V3: 3-way valve outside of vapouriser
normally I1 to O
when switched I2 to O (taking additional dry air during analyser loading, valve mask 14)
V4: Needle valve, for flow regulation of inlet pump

Figure S2: ATR sampling schematic. The red arrow depicts the sample flow (through a heated 10 mm ID PTFE line) from the rearward-facing gooseneck inlet to a Picarro vaporizer, which was attached to the Picarro L2130-i water vapor isotopic analyzer on the aircraft. A 0.2 µm PTFE vent filter was installed at the top of the inlet line to prevent particles from entering the laser spectrometer. Valves inside the vaporizer determined whether the analyzer sampled ambient water vapor or calibration standards, which were pumped into the vaporizer by a Picarro Standards Delivery Module (SDM). SP1 and SP2 represent the two liquid standards delivered by the SDM.

Text S1. BCO calibration results

Calibration measurements, standard deviations, and target (reference) values for the oxygen and hydrogen isotope ratios of the two water vapor isotopic analyzers installed at the BCO are provided in the accompanying spreadsheet *BCO_Cals.xlsx*. *L115* refers to the Picarro CRDS system, and *LGR* refers to the Los Gatos Research OA-ICOS system. Other abbreviations include *m* for measured, *s* for standard deviation, *cal* for calibrated, *err* for error, *diff* for difference, and *ref* for reference.

A post-campaign laboratory test of the CRDS system's isotopic dependence on water vapor concentration was conducted using a bubbler system (cf. Ellehoj et al., 2013). The test found root mean square differences between isotopic measurements at a reference humidity value (20,000 ppmv) and measurements at seven higher humidities (spanning 20,000 to 35,000 ppmv) of just 0.1‰, 0.4‰, and 1.0‰ for $\delta^{18}O$, δD, and *d*, respectively. Therefore, no humidity-dependent correction was applied to the BCO CRDS data.

The humidity dependence of the OA-ICOS isotopic measurements during EUREC^{4}A was not explicitly characterized; however, subsequent comparisons with the CRDS data suggest a remnant humidity bias may affect the OA-ICOS isotope ratios (Fig. S3). Data users desiring to use the OA-ICOS measurements to gap-fill the BCO CRDS time series may consider scaling the OA-ICOS data. This can be done by applying a mean offset or by means of a regression model (Fig. S4-S5), though more complex adjustments are also justifiable.

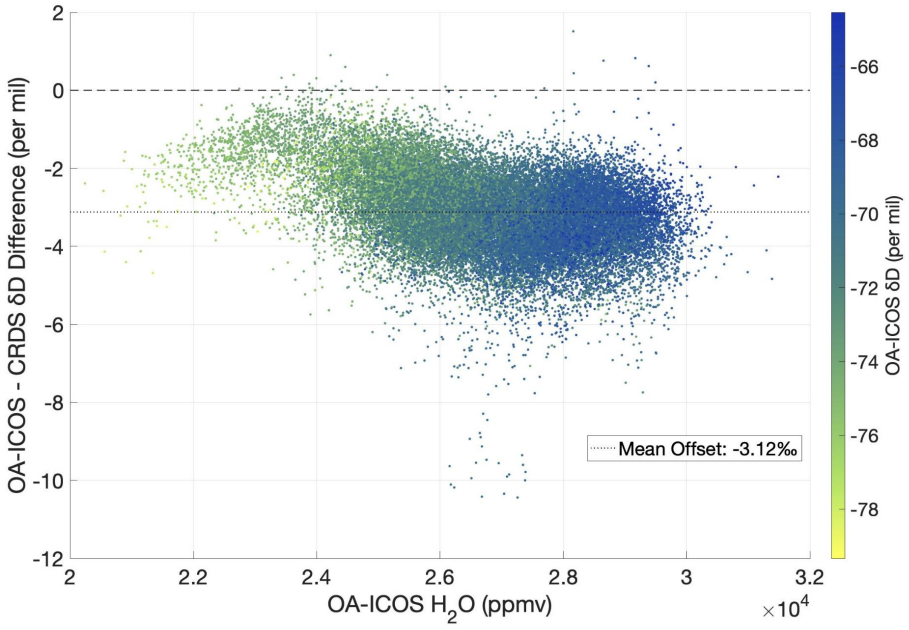

Figure S3: Isotopic differences between BCO analyzers as a function of humidity. Differences in δD (‰) between the Los Gatos Research (LGR) OA-ICOS analyzer and the Picarro CRDS analyzer (y-axis) increase with humidity (x-axis; represented by the OA-ICOS water vapor mole fraction (ppmv)), suggesting a bias in the OA-ICOS isotopic data. Shading shows the OA-ICOS normalized and drift-corrected δD value in units ‰.

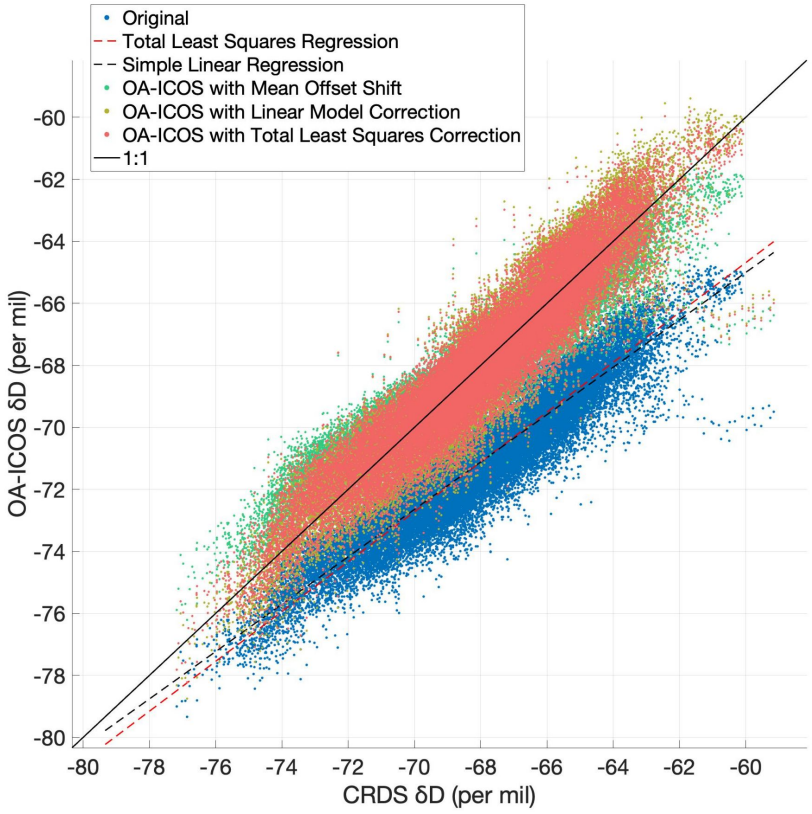

Figure S4: OA-ICOS scaling examples. Isotopic data from the BCO OA-ICOS analyzer can be scaled to the CRDS isotope ratios either by applying a simple offset or a linear correction model. The scatterplot shows the original relationship between the (normalized and drift-corrected) OA-ICOS and CRDS δD values (blue dots). It also shows how the relationship shifts towards the 1:1 line (black, solid) when the OA-ICOS data are scaled by one of three methods: a simple offset (green dots), a simple linear regression (red dashed line, gold dots), or a total least squares regression (black dashed line, orange dots).

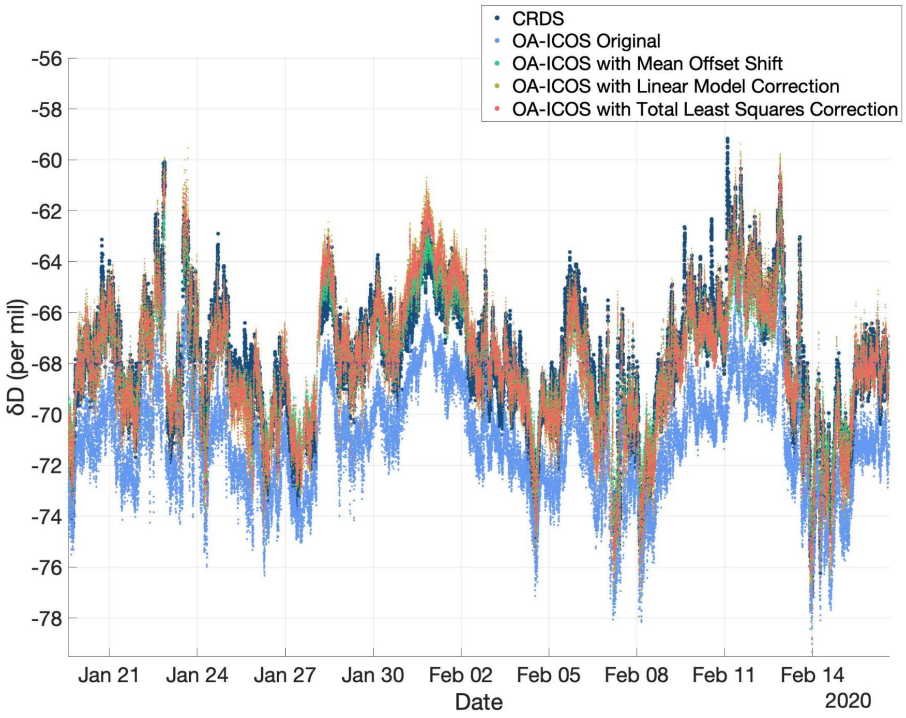

Figure S5: BCO time series comparison. After scaling the original OA-ICOS data (light blue dots) to the CRDS data by one of the methods illustrated in Fig. S4, the adjusted δD (‰) time series (green, gold, or orange dots) converges with the CRDS δD time series (dark blue dots).

Text S2. ATR calibration results

Calibration measurements, standard deviations, and target (reference) values for the three standard waters (*STD*) run on the water vapor isotopic analyzer installed aboard the ATR are provided in the accompanying spreadsheet *ATR_Cals.xlsx*. Abbreviations are the same as described in Text S1. Functions to correct the isotopic dependence on humidity (*WVDC*), to normalize the isotope ratios to the VSMOW-SLAP (Vienna Standard Mean Ocean Water - Standard Light Antarctic Precipitation) scale, and to correct the measured water vapor concentrations are also provided. A schematic of the bubbler system used to determine the humidity-dependence correction is provided in Fig. S6.

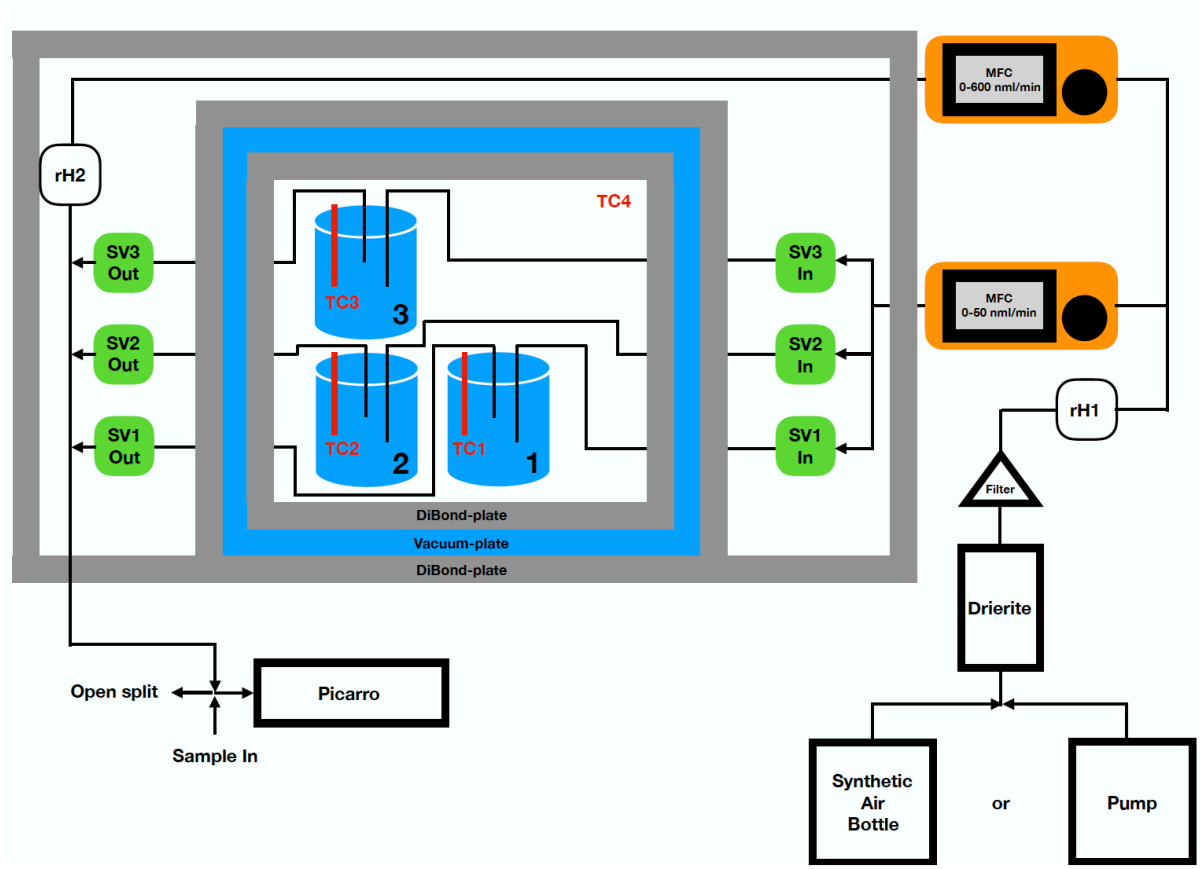

Figure S6: ATR calibration bubbler schematic. In the black pearl bubbler system used to test the humidity dependence of the isotopic measurements of the ATR analyzer (Picarro), dry air is pumped through a Drierite drying unit and separated into two streams, whose flow is controlled by two mass flow controllers (MFC, orange). One dry air stream is directed through one of three 2 L liquid standard bottles (blue). Upon passage through the bottles, the air becomes saturated in water vapor. The temperature at various points (TC 1-4) inside an isolated box, made of DiBond plates (gray) with vacuum in between, is measured to keep track of potential changes in fractionation coefficients. The saturated stream is then mixed with various amounts of dry air from the second stream, whose relative humidity is monitored at location rH2. rH1 verifies the dryness of air supplied to the system.

Text S3. P-3 calibration results and uncertainty estimates

The humidity dependence of the isotopic measurements made on the P-3 aircraft was tested by diluting a moisture source of known isotopic composition to varying degrees with dry air. The dependence was checked twice before the EUREC^{4}A winter 2020 field deployment, three times shortly following the deployment, and once just over one year later. Although substantial deviations in the measured isotope ratios were detected for water vapor concentrations less than 1000 ppmv, the direction and magnitude of the deviations varied depending on the isotopic composition of the calibration source relative to the isotopic composition of the water vapor sampled immediately prior. Because these variations (some of which transpired within a single 24 hour period) could be approximated crudely using a simple linear mixing model, we hypothesize that the reference gases used to test the humidity dependence were contaminated with water vapor that had desorbed from the tubing and valve surfaces of the

calibration system. Such contamination prevented an accurate characterization of humidity-dependent isotopic biases.

Following guidance from the National Institute of Standards and Technology (NIST, 2021) for situations in which an "inconsistent" bias is detected, no humidity-dependent correction was applied to the P-3 isotopic field measurements. Instead, the spread in the calibration measurements was used to estimate uncertainty in the humidity dependence of the field data. To quantify this spread, the residual standard deviation (in units ‰) was calculated for humidity bins with centers at 50, 100, 200, 300, 400, 500, 600, 700, 800, 900, 1000, 1200, 1400, 1600, 1800, 2000, 2400, 2800, 3200, 3600, 4000, 4400, and 4800 ppmv. Modified third and second order polynomials were then fit to these standard deviations (as a function of the natural log of water vapor concentration) and then flattened for humidity values exceeding 1000 and 2000 ppmv, for $\delta^{18}O$ and δD, respectively. The polynomial fits were then used to predict uncertainties at all humidity values measured in the field.

Normalization of the P-3 isotopic measurements to the VSMOW-SLAP scale was accomplished by fitting a linear regression between the measured and known values of four liquid water standards, which were introduced to the analyzer soon after the field deployment. These standards had values of -45.41, -22.38, -14.15, and -0.28 ‰ for $\delta^{18}O$ and -355.18, -163.50, -111.65, and 1.60 ‰ for δD. Each standard was injected into a Picarro vaporizer multiple times. To minimize biases associated with hysteresis, the first 5-to-6 injections of each standard were ignored and the remaining 4-to-8 averaged to produce a single measured value. Only the last ~2 minutes of each injection were considered in the averaging. The calibration resulted in the following linear normalization functions:

$$\delta^{18}O_{cal} = 0.785 + 1.137 \times \delta^{18}O_{meas} \quad (1)$$

$$\delta D_{cal} = -4.083 + 0.936 \times \delta D_{meas} \quad (2)$$

where the subscripts *cal* and *meas* represent the calibrated (normalized) and measured isotope ratios, respectively. The residual standard deviations of the linear regression fits are 0.08 ‰ for $\delta^{18}O$ and 0.73 ‰ for δD.

Linear correction functions derived from normalization checks performed in the field were only used to evaluate uncertainty rather than to adjust the isotopic measurements. Liquid standards used during the in-field calibration checks were the same as those used in the post-campaign calibration except for the most enriched standard (whose in-field value was -2.17 ‰ in $\delta^{18}O$ and -8.60 ‰ in δD). Much like before, the first 2-to-3 injections were ignored and the subsequent 2-to-4 injections aggregated to derive a single calibration measurement. However, because a leak was suspected in the vaporizer used in the field, only the first minute of each injection was considered for analysis, and the median (rather than mean) was used to produce a single measured value. Comparing the normalization curves derived post-campaign with those suggested by the in-field checks resulted, over the range of standard values, in maximal (absolute) correction differences (i.e. *max_difference*) of 0.99 ‰ in $\delta^{18}O$ and 3.19 ‰ in δD. The potential errors in the normalization are thus taken as $\frac{1}{\sqrt{3}} \times max\_difference$. Adding these errors in quadrature with the residual standard deviations from the humidity-dependent tests provides an estimate of total uncertainty in the P-3 calibrations. Because (normalization) corrections are applied to the sample-rate data, total calibration uncertainties are propagated (and reduced) when the sample-rate data are averaged to 1 s.

In addition to the reported calibration uncertainty associated with each 1 s isotope ratio (e.g. $\delta^{18}O_u$), there is also a standard error associated with averaging the sample-rate measurements. The so-called standard error of the mean can be calculated from the standard deviations (e.g. $\delta^{18}O_{sd}$) and number of sample-rate points per average (n) provided in the 1 Hz data files. That said, data users wishing to be especially cautious in their analyses may wish to use the standard deviations, rather than the standard errors or reported calibration uncertainties, as a more conservative measure of total uncertainty.

Water vapor concentrations from the P-3 isotopic analyzer were corrected independently by applying the following correction function, derived from the calibration measurements:

$$H_2O_{cal} = H_2O_{meas} - [1.615\times10^{-2}(H_2O_{meas}) - 1.573\times10^{-6}(H_2O_{meas})^2]. \quad (3)$$

Uncertainties in the water vapor concentration were estimated from the standard errors of prediction associated with the quadratic fit.

Table S1. Liquid standard values and their uncertainties for Meteor water vapor measurements (units ‰).

	$\delta^{18}O$		δD	
Standard	**value**	**uncertainty**	**value**	**uncertainty**
1	-3.26	0.12	-13.12	0.57
2	-2.79	0.12	-17.44	0.56
3	-17.85	0.16	-132.23	0.82
4	-20.97	0.16	-158.13	0.82

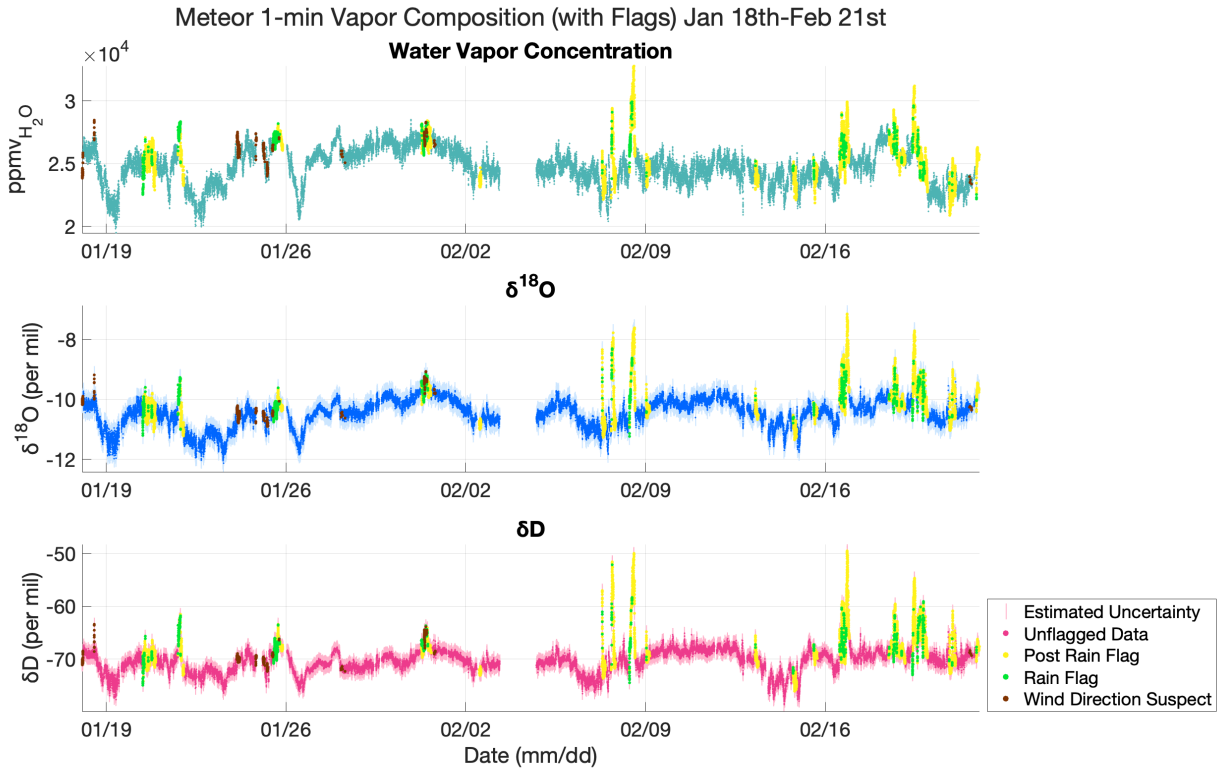

Figure S7: Meteor quality control flags. Water vapor concentration and water vapor isotopic time series from the Meteor are marked with flags for periods of rainfall (green circles), for the three hours post rain (yellow circles), when isotopic values exhibit large deviations due to precipitation processes and/or rain evaporating from ship surfaces, and for periods when the wind direction relative to the ship may have caused contamination by ship emissions (brown circles).

References

Ellehoj, M. D., Steen-Larsen, H. C., Johnsen, S. J., and Madsen, M. B.: Ice-vapor equilibrium fractionation factor of hydrogen and oxygen isotopes: Experimental investigations and implications for stable water isotope studies, Rapid Commun. Mass Sp., 27, 2149–2158, doi:10.1002/rcm.6668, 2013.

NIST/SEMATECH e-Handbook of Statistical Methods, https://doi.org/10.18434/M32189, 2021.